Electronic Supplementary Material (ESI) for New Journal of Chemistry.

A naked-eye colorimetric sensor based on chalcone for sequential recognition of copper (II) and sulfide in semi-aqueous solution: Spectroscopic and Theoretical approaches

Nidhi Singh[1], Ramesh Chandra[1,2*]

[1]Department of Chemistry, University of Delhi, Delhi 110007, India

[2]Dr .B. R. Ambedkar Center for Biomedical Research, University of Delhi, Delhi 110007, India

*****Corresponding author:
Prof. Ramesh Chandra,
Drug Discovery & Development Laboratory,
Department of Chemistry, University of Delhi and
Dr.B.R.Ambedkar Center for Biomedical Research,
University of Delhi, Delhi- 110007, India
Email: rameshchandragroup@gmail.com, acbrdu@hotmail.com

Figure S1. Benesi Hilderbrand plot of A01 (Absorbance at 504 nm) assuming 1:1 stoichiometry of A01-Cu^{2+} complex.

Figure S2. Modified Benesi Hilderbrand plot of A01 (Absorbance at 504 nm) assuming 2 :1 stoichiometry of A01-Cu^{2+} complex

Figure S3. Benesi Hilderbrand plot of A01 (Absorbance at 504 nm) assuming 1:2 stoichiometry of A01-Cu^{2+} complex.

Figure S4. Job plot of A01 and Cu^{2+} in CH_3CN-H_2O (1:1, v/v; HEPES, 20 mM; pH = 7.4), the total concentration of [Cu^{2+}] and [A01]) is 40μM.

Figure S5. Determination of the detection limit of A01 (40 μM) for Cu^{2+} based on change of absorbance at 504 nm.

Figure S6. Absorption spectra of A01 (40 μM) in the presence of different salts of copper (40 μM) in CH_3CN-H_2O (1:1, v/v; HEPES, 20 mM; pH = 7.4).

Figure S7. Reversible absorption spectral changes of A01 (40 μM) after sequential addition of Cu^{2+} (1.0 eq.) and EDTA (1.0 eq.) in CH_3CN-H_2O (1:1, v/v; HEPES, 20 mM; pH = 7.4).

Figure S8. Determination of the detection limit of A01-Cu^{2+} (40 μM) for S^{2-} based on change of absorbance at 504 nm.

Figure S9. Optimized structure of A01.

Figure S10. HOMO and LUMO surfaces of optimized structure A01 and their respective energy values.

Table S1. Various global reactivity indices (in eV) of A01 in the gas phase.

Figure S11. Molecular electrostatic potential map of A01

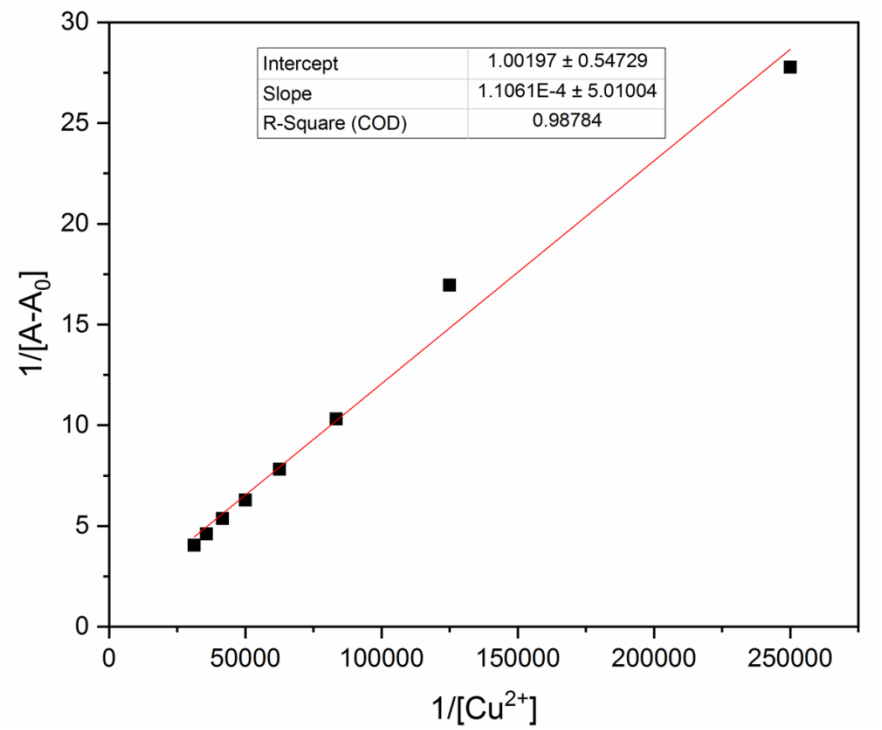

Figure S1. Benesi Hilderbrand plot of A01 (Absorbance at 504 nm) assuming 1:1 stoichiometry of A01-Cu^{2+} complex.

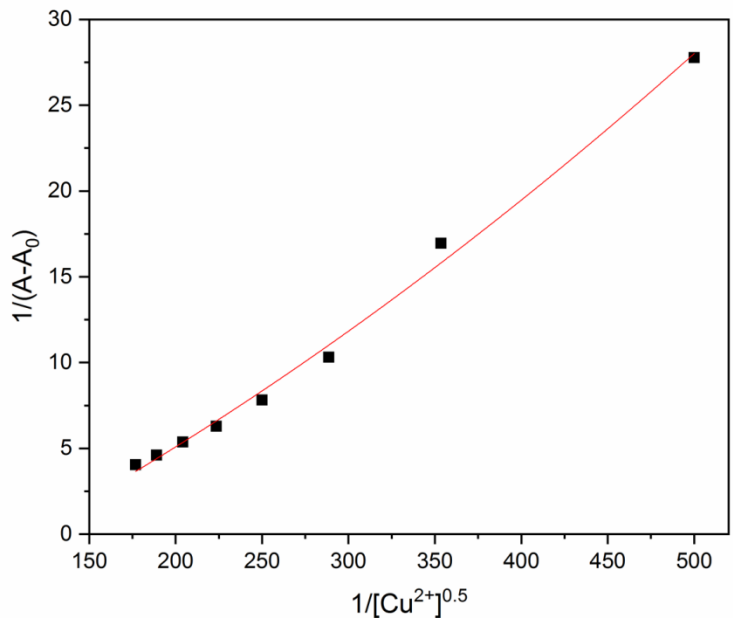

Figure S2. Modified Benesi Hilderbrand plot of A01 (Absorbance at 504 nm) assuming 2 :1 stoichiometry of A01-Cu^{2+} complex

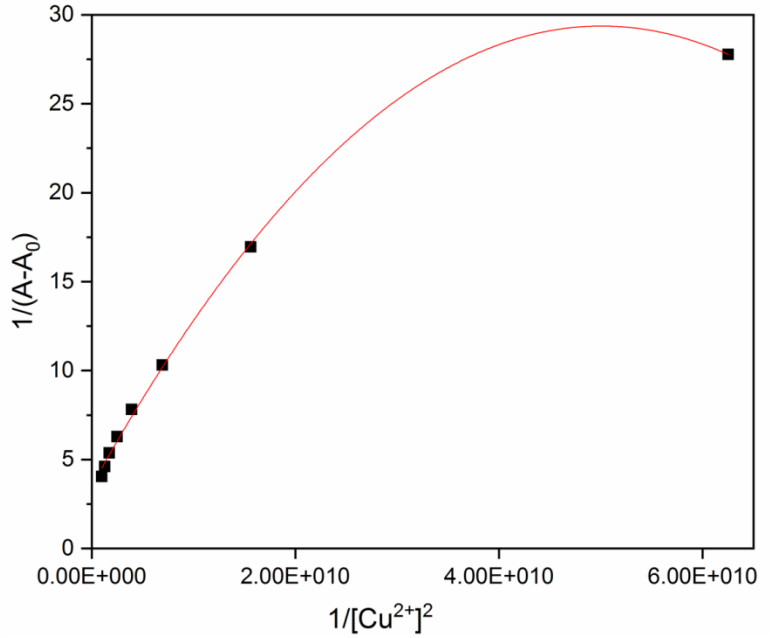

Figure S3. Benesi Hilderbrand plot of A01 (Absorbance at 504 nm) assuming 1:2 stoichiometry of A01-Cu^{2+} complex.

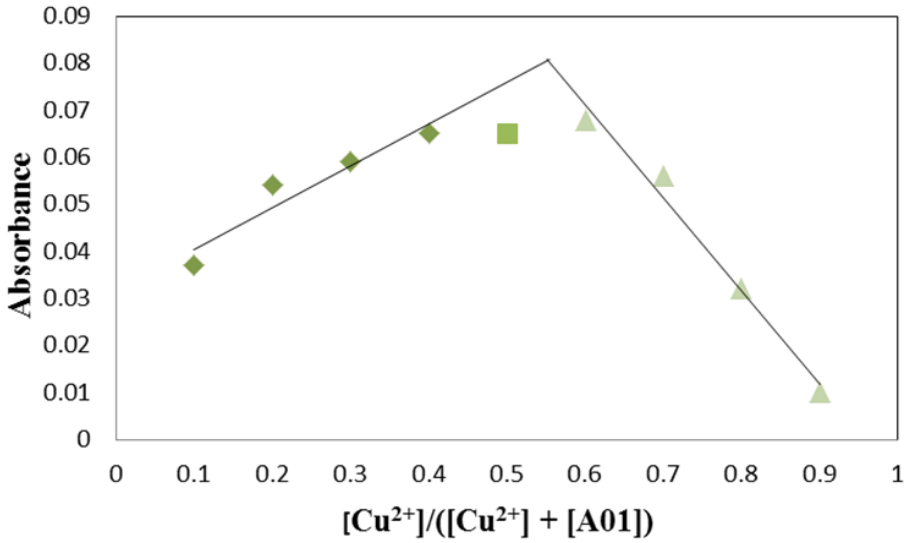

Figure S4. Job plot of A01 and Cu^{2+} in CH_3CN-H_2O (1:1, v/v; HEPES, 20 mM; pH = 7.4), the total concentration of [Cu^{2+}] and [A01]) is 40μM.

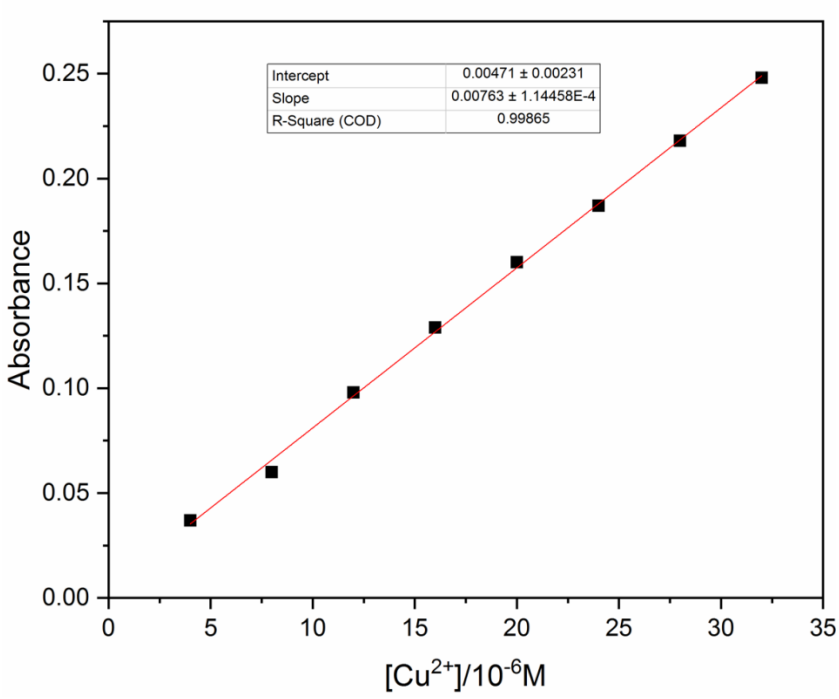

Figure S5. Determination of the detection limit of A01 (40 μM) for Cu^{2+} based on change of absorbance at 504 nm.

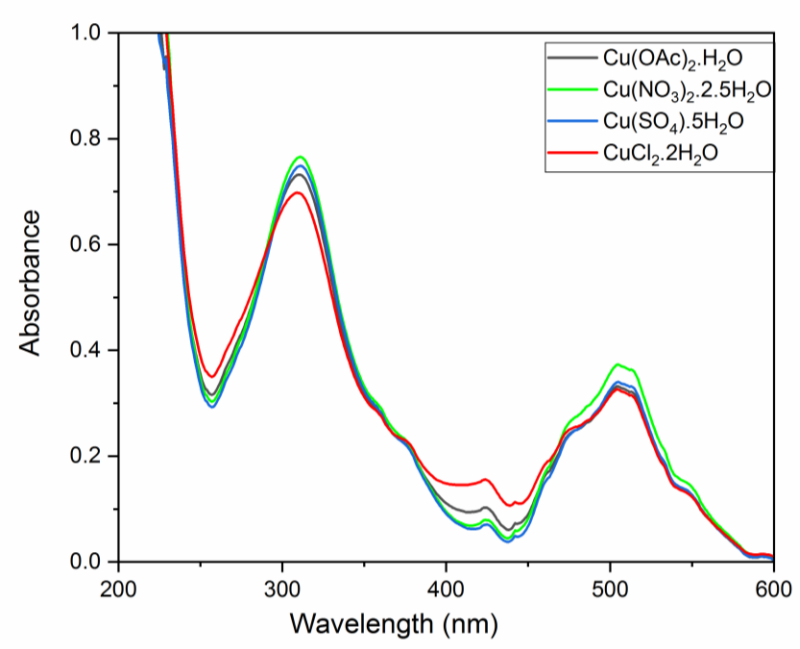

Figure S6. Absorption spectra of A01 (40 μM) in the presence of different salts of Copper (40 μM) in CH_3CN-H_2O (1:1, v/v; HEPES, 20 mM; pH = 7.4).

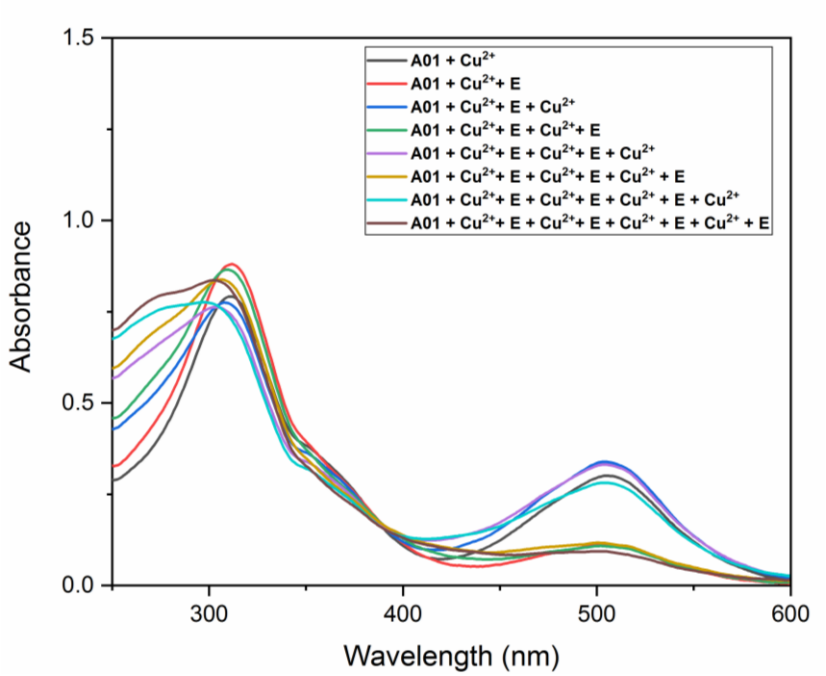

Figure S7. Reversible absorption spectral changes of A01 (40 μM) after sequential addition of Cu^{2+} (1.0 eq.) and EDTA (1.0 eq.) in CH_3CN-H_2O (1:1, v/v; HEPES, 20 mM; pH = 7.4).

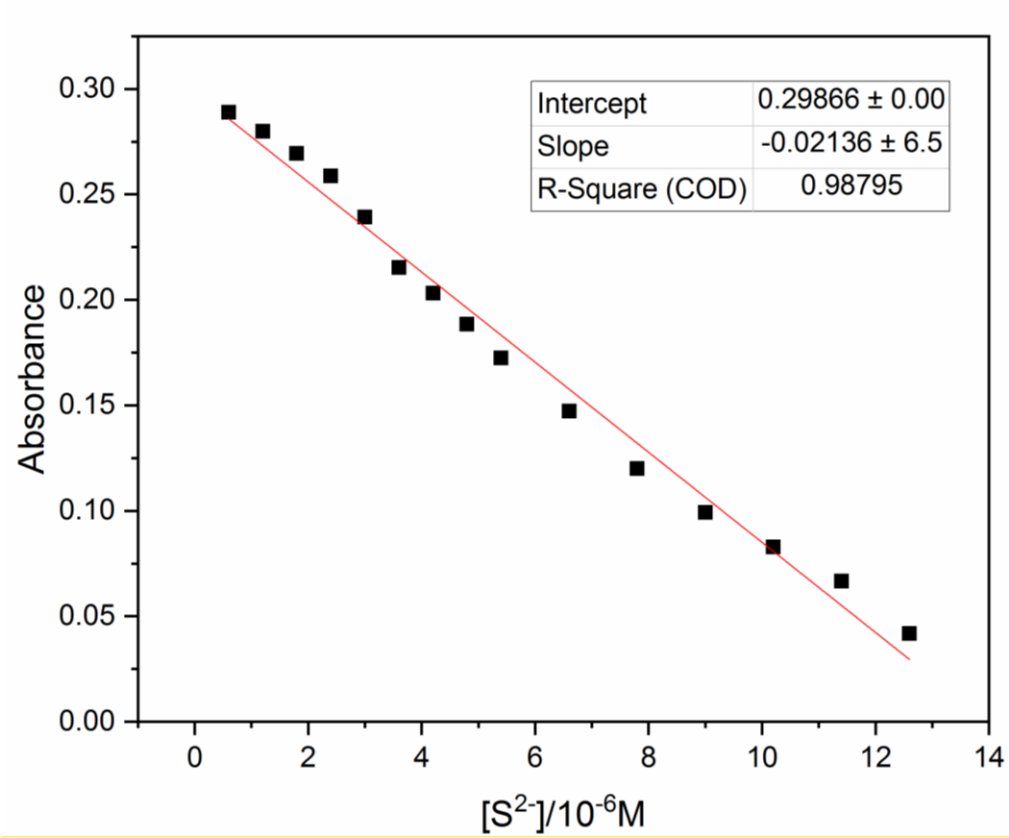

Figure S8. Determination of the detection limit of A01-Cu^{2+} (40 μM) for S^{2-} based on change of absorbance at 504 nm.

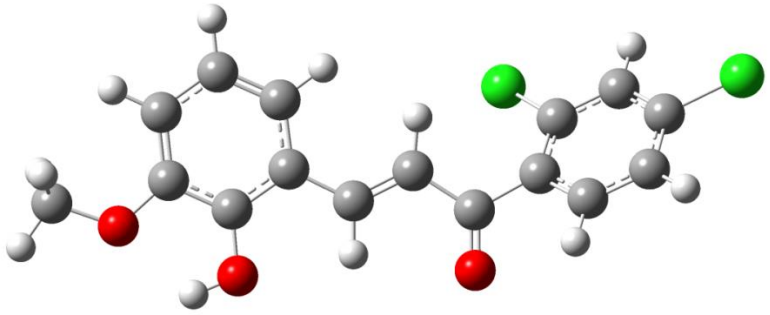

Figure S9. Optimized structure of A01

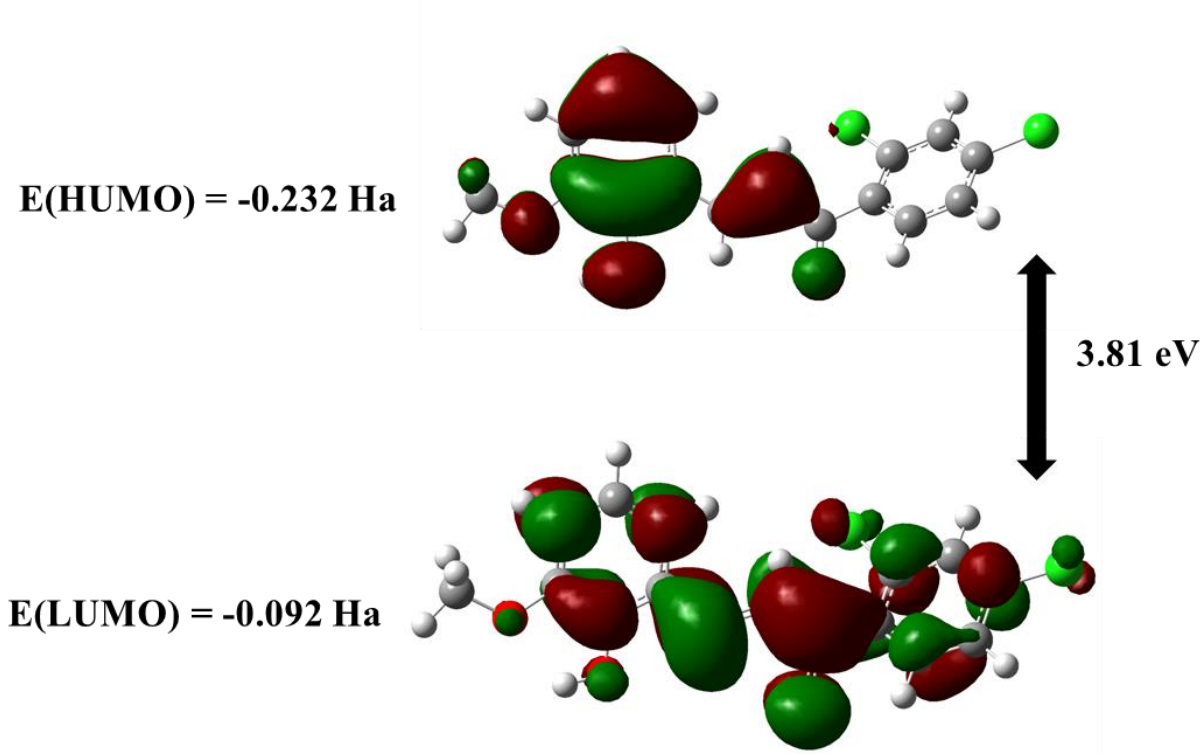

Figure S10. HOMO and LUMO surfaces of optimized structure A01 and their respective energy values.

Table S1. Various global reactivity indices (in eV) of A01 in the gas phase

Parameters	**B3LYP**
Vertical ionization potential (IP)	6.31
Electron affinity (EA)	2.50
Chemical hardness (η)	1.90
Chemical potential (μ)	-4.41
Electrophilicity index(ω)	5.10

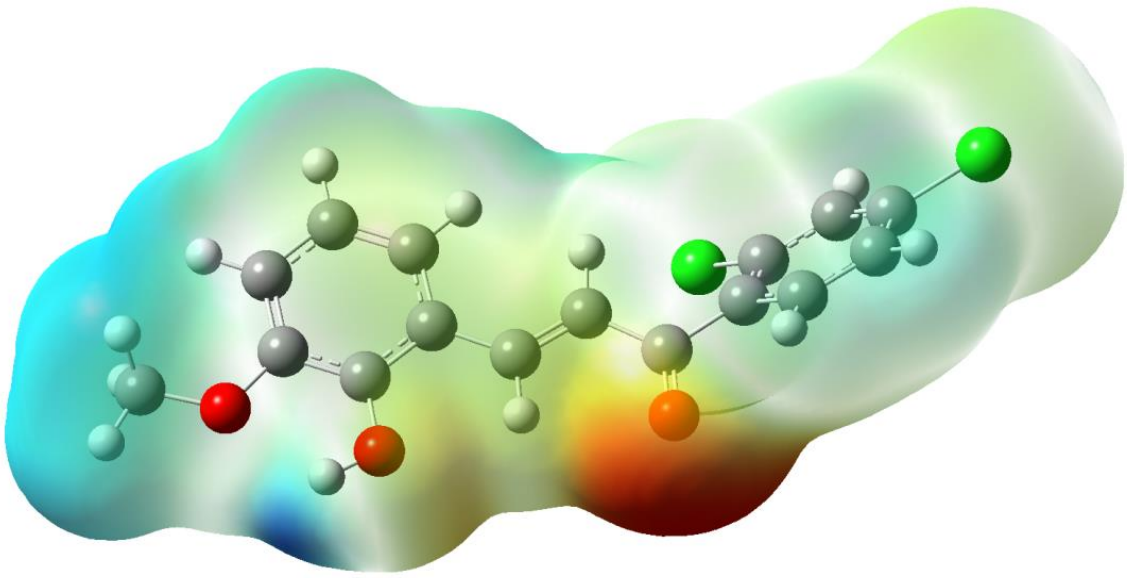

Figure S11. Molecular electrostatic potential map of A01